International Journal of Research and Reviews in Pharmacy and Applied science

www.ijrrpas.com

THE EFFECT OF SOOT AND WATER SOLUBLES IN RADIATIVE FORCING OF URBAN AEROSOLS

B. I. Tijjani[1] and D. O. Akpootu[2]

[1]Department of Physics, Bayero Univerisity, Kano, idrith@yahoo.com

[2]Department of Physics, Usmanu Danfodiyo University, Sokoto, profdon03@yahoo.com

ABSTRACT

In this paper the optical depths, asymmetry parameters and single scattering albedos of urban aerosols were modeled using OPAC by altering the number densities of soot and water soluble at the spectral range of 0.25 μm to 1.0μm at relative humidities (RHs) 0, 50, 70, 80, 90, 95, 98 and 99%. The data was used to calculate the radiative forcings(RF) and Angstom parameters. For the RF it was observed that as the RH increases there is a small increase in warming from 0 to 70% but as from 80 to 99% RH there is an increase in cooling as we moved from the first to the second and then to the third model. The spectral distributions of AOD have been used to derive Angstom parameters and this help us to determine the nature of the aerosols size distribution and increase in RH shows increase in mode size distributions. Using regression analysis, the Angstrom exponents were determined along with α_1 and α_2, the coefficients of a second order polynomial fit. The analysis further shows that these aerosols have bimodal type of particle distributions with Junge type as dominant.

INTRODUCTION

Atmospheric aerosol particles are one of the most variable components of the Earth's atmosphere, and are known to influence the energy budget and climate. Aerosol particles affect the Earth's radiative balance and climate directly by absorbing and scattering solar radiation (Haywood and Shine, 1997; Forster et al., 2007), and indirectly by acting as cloud condensation nuclei, changing thus the microphysical properties of clouds (Kaufman et al., 2005; Forster et al., 2007).

A significant fraction of atmospheric aerosols is comprised of carbonaceous materials, which are often categorized as elemental or black/graphitic carbon (EC/BC) and organic carbon (OC). They are in airborne particulate matters that originate from the incomplete combustion of carbonaceous fuel (of fossil fuels, biomass and agricultural wastes and forest fires) (Salako et al., 2012; Jacobson, 2001). These forms of carbon play an important role in climate change, either contributing to or offsetting atmospheric warming (Hansen and Sato, 2001; Menon et al., 2002; Ramanathan et al. , 2001). BC has attracted special attention because of its significant influence on climate change as well as its adverse effects on human health (Kim et al., 2011; Myhre et al., 1998; Jacobson, 2001). BC is chemically inert and mostly in the accumulation (submicron) size regime, and has a long atmospheric lifetime (of several days to weeks) depending on the meteorological conditions (Reddy and Venkataraman, 1999; Babu and Moorthy, 2002) and hence is amenable for long-range transport (Moorthy and Babu, 2006). The bulk of BC aerosols (~90%) resides in the PM2.5 (particulate matter having diameter ≥ 2.5 μm) fraction (Viidanoja et al., 2002; Cao et al., 2009). Excessive PM2.5 concentrations have been shown to negatively affect the respiratory and cardiac health of humans (e.g., Park et al., 2002) and also reduce visibility. Coal and biomass burning, vehicle exhaust and industrial emissions all contribute to the ambient PM and a clear inverse relationship is noticed between BC concentrations and rainfall in this area (.Kumar et al., 2012). The Intergovernmental Panel on Climate Change (IPCC) has estimated that the global mean clear-sky radiative forcing of BC is 0.23 ± 0.25 W/m^2 (IPCC, 2007), which is approximately half the value of Methane, the second most important greenhouse gas after Carbon dioxide. On a global basis BC contributes ~0.5 W/m2 to radiative forcing (Jacobson, 2001). BC may also have regional climatic impacts. For example, Menon et al. (2002) have suggested that the high concentrations of soot over India and China are responsible for a trend toward increased flooding in the south and drought in the north. It is estimated that the reduced atmospheric transparency caused by high soot concentrations over India and China decreases agricultural productivity by 10–20% (Chameides et al., 1999). Soot deposited on plant leaves also reduces plant productivity (Bergin et al., 2001).

In the context of climatic research most attention has been paid to sulphate aerosols among the tropospheric aerosols due to scattering of solar radiation (Myhre et al., 1998). Aerosol particle types which contribute to the scattering coefficient include organic particles, water-soluble inorganic species such as sulphates, nitrates etc. that are produced by conversion from SO_2 and NO_x associated mainly with fossil fuel/biomass combustion, and ammonium from fertilizers and biological sources.

Haywood et. al., (1997) and Hansen et al., (1997) show that a mixture of soot and sulphate aerosols may further increase the importance of the absorption by soot aerosols and depending on their composition, can cause either cooling or warming of the atmosphere.

As the soot particles age in the atmosphere, they are mixed with other particles like sulphates through coagulation, condensation of secondary aerosols compounds and cloud processing. Over a timescale of a few days, the aging process eventually leads to an internal aerosol mixture. (Seinfeld and Pandis, 1998).

To be able to analyse and understanding the influence of atmospheric aerosol on climate, visibility and photochemistry requires knowledge of their optical and physical properties, such as the optical depth, single scattering albedo, upscatter fraction (fraction of incident solar radiation that is scattered upward to space), composition and size distribution (e.g. Waggoner et al., 1981; Haywood and Boucher, 2000; Alados-Arboledas et al., 2003; Alados-Arboledas et al., 2008). All these properties can be greatly influenced by hygroscopic growth as a result of the change in RHs (Mikhailov et al., 2006; Garland et al., 2007).

In this paper the optical depths, asymmetry parameters and single scattering albedo of urban aerosols were modeled by altering the number densities of soot and water soluble at the spectral range of 0.25 μm to 1.0μm at relative humidities (RHs) 0, 50, 70, 80, 90, 95, 98 and 99% using Optical Properties of Aerosol and Clouds software. The RF and Angstrom coefficients were calculated. The Ångström coefficient was used to characterizes the dependence of AOD on wavelength and provides information about the size of aerosol particles. Finally, the spectral behaviours asymmetry parameters were analysed to understand the nature of the forward scattering of these particles as a result of these changes.

METHODOLOGY

	Model1	Model2	Model3
components	No. density (cm^{-3})	No. density (cm^{-3})	No. density (cm^{-3})
Insoluble	1.5	1.5	1.5
water soluble	25,000.0	30,000.0	35,000.0
Soot	110,000.0	120,000.0	130,000.0
total	135,001.5	150,001.5	165,001.5

Table 1: Compositions of aerosols types (Hess et al., 1998)

Although a fully exact radiative transfer model is difficult, so in this paper we used the approach of Chylek and Wong (1995) where they show that the direct aerosol radiative forcing at the top of the atmosphere can be approximated by

$$\Delta F_R = -\frac{S_0}{4} T_{atm}^2 (1 - N_{cloud}) 2\tau\{(1 - A)^2 \beta\omega - 2A(1 - \omega)\} \quad (1)$$

Where S_0 =1368Wm^{-2} is a solar constant, T_{atm}=0.79 is the transmittance of the atmosphere above the aerosol layer, N_{cloud}=0.6 is the fraction of the sky covered by clouds, the global averaged albedo A=0.22 over land, β is the fraction of radiation scattered by aerosol into the atmosphere and τ the optical thickness (Penner et al., 1992). The above expression gives the radiative forcing due to the change of reflectance of the earth-aerosol system. The upscattering fraction is calculated using an approximate relation (Sagan and Pollack, 1967)

$$\beta = \frac{1}{2}(1 - g) \quad (2)$$

where g is the asymmetry parameter. Although the model is simple but was used to provide reasonable estimates for the radiative forcing by both sulfate aerosols (Charlson et al., 1992) and absorbing smoke aerosols Chylek and Wong (1995).

The spectral behavior of the aerosol optical thickness, with the wavelength of light (λ) is expressed as inverse power law (Angstrom, 1961):

$$\tau(\lambda)=\beta\lambda^{-\alpha} \quad (3)$$

where β is the turbidity and α is the Angstom exponent (Liou, 2002; O'Neill and Royer, 1993). The formula is derived on the premise that the extinction of solar radiation by aerosols is a continuous function of wavelength, without selective bands or lines for scattering or absorption (Ranjan et al., 2007).

The wavelength dependence of τ(λ) can be characterized by the Angstron parameter, which is a coefficient of the following regression:

$$\ln\tau(\lambda) = -\alpha\ln(\lambda) + \ln\beta \quad (4)$$

The Angstrom exponent itself varies with wavelength, and a more precise empirical relationship between aerosol extinction and wavelength is obtained with a 2nd-order polynomial (King and Byrne, 1976; Eck et al., 1999; Eck. et al., 2001a, b, 2003; Kaufman, 1993;O'Neill et al., 2001a, 2003) as:

$$\ln\tau(\lambda) = \alpha_2(\ln\lambda)^2 + \alpha_1\ln\lambda + \ln\beta \quad (5)$$

Here, the coefficient α_2 accounts for a "curvature" often observed in sunphotometry measurements. In case of negative curvature ($\alpha_2<0$, convex type curves) the rate of change of α is more significant at the longer wavelengths, while in case of positive curvature ($\alpha_2>0$, concave type curves) the rate of change of α is more significant at the shorter wavelengths (Kaufman, 1993; Eck et al., 1999; Eck. et al., 2001b; Reid et al., 1999). Eck et al. (1999) reported the existence of negative curvatures for fine-mode aerosols and positive curvatures for significant contribution by coarse-mode particles in the size distribution.

RESULTS AND OBSERVATIONS

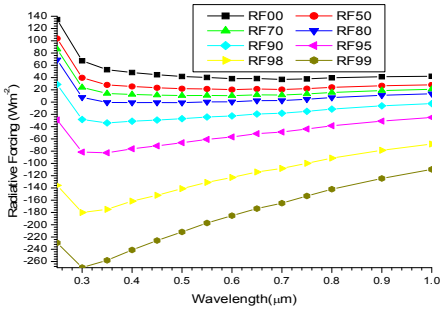

Figure1a: A graph of radiative forcing against wavelength

Its relation with wavelengths at 0% RH shows that it is more dependent at shorter wavelength. It shows a sharp fall at 0.25 to 0.3 but from 0.3 to 1.0 it becomes almost a straight line with very small negative slope. As the RH increases, the nature at 0.25 to 0.3 the steepness decreases but as the spectral interval of 0.3 to 1.0 the slope continues to decrease and subsequently becomes positive. Its relation with RH shows that the cooling is increasing with the increase in RH.

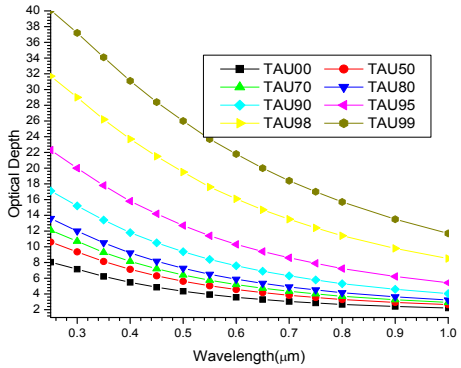

Figure 1b. A graph of optical depth against wavelength

Figure 1b shows that optical depths follow a relatively smooth decrease with the increase in wavelengths though some are steeper than others and the steepness increases with the increase in RHs. It is evident from the figure that there is a relatively strong wavelengths dependence of optical depths at shorter wavelengths that decreases toward longer wavelengths irrespective of the RH, attributing to the presence of fine and coarse particles. The presence of fine mode particles which are selective scatters enhanced the irradiance scattering in shorter wavelength only while the coarse mode particles provide similar contributions to the optical depths at both wavelengths (Schuster et al., 2006). Additionally fine particles scatter more lights in the forward direction than coarse particles.

In relation to RH, it shows that optical depths increase with the increase in RH. As the RH increases the optical depths continue to increase due to the increase in concentration of fine mode particles as a result of the continue sedimentation of coarse particles due to the increase in RH. And also as the RH increases there is an increase in hygroscopic growth more to fine particles than coarse particles and since fine particles scatter more lights in the forward direction than coarse particles, that is why the optical depth are higher at shorter wavelengths than longer wavelengths even at higher RHs. These hygroscopic growth behaviors also reveal an immense potential of light scattering enhancement in the forward direction at high humidities and the potential for being highly effective cloud condensation nuclei.

It also shows monomode type of particle size distributions in the form of Junge power law in this spectral range (Eck et al., 1999) and increase in RH has caused increase in mode growth because of the increase in optical depths. The increase of AOD with RH at the delequicence point (90 to 99%) is that the growth increase substantially, making the process strongly nonlinear with RH(Fitzgarald, 1975; Tang, 1996).

Linear				Quadratic			
RH(%)	R^2	A	B	R^2	α_1	α_2	β
0	0.99752	0.97817	2.17621	0.99792	-1.04481	-0.04888	2.14480
50	0.99670	1.04467	2.65697	0.99873	-1.20585	-0.11824	2.56516
70	0.99566	1.06295	2.97715	0.99900	-1.27306	-0.15413	2.84376
80	0.99445	1.07225	3.33467	0.99923	-1.32618	-0.18628	3.15496
90	0.99143	1.07173	4.26453	0.99954	-1.40306	-0.24305	3.96716
95	0.98697	1.04311	5.84636	0.99978	-1.44912	-0.29784	5.35079
98	0.97953	0.96733	9.36627	0.99993	-1.44427	-0.34987	8.44072
99	0.97340	0.89938	13.06814	0.999974	-1.40703	-0.3724	11.69813

Table 2: The results of the Angstrom coefficients for Model1 using equations (4) and (5) at the respective relative humidities using regression analysis with SPSS16.0.

By the value of $\alpha \cong 1$ indicates the dominance of fine particles and is verified by the sign of α_2 from the quadratic part. The value of α continues to increase with RH upto 80% and α_2 continues to increase in magnitude which indicates that increase in RH has caused increase in α as well as the increase in the curvature. But as from 90% RH the α started decreasing and then continues to decrease with the increase in RH. This shows that 90 to 99% is the delinquent point of this mixture and that at this point the particles behave as if large particle despite the fact that α_2 continues to increase.

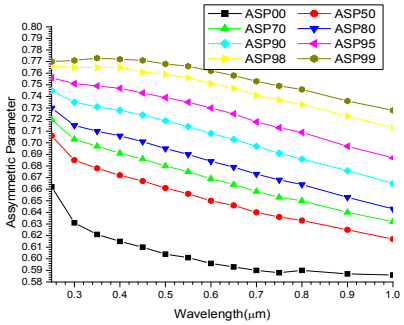

Figure 1c. A graph of asymmetric parameter against wavelength

It relation with wavelength satisfies power law. But as the RH increases the exponent continues to decrease up to the extent that it becomes positive. Its relation with RH shows that it is increasing with the increase in RH. This implies that hygroscopic growth enhances scattering more in the forward and this implies the dominance of fine particles because hygroscopic growth has more effect on fine particles.

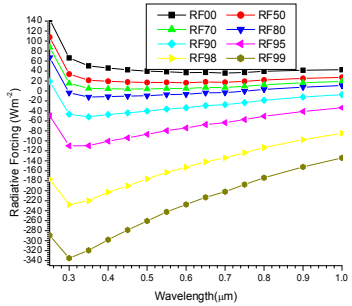

Figure 2a. A graph of radiative forcing against wavelength

It has similar behavior with that of 1a, but the main difference is that there is an increase in RF(warming) at 0 and 50% but at 70 no much change and as the RH increase we see that the forcing (warming) is decreasing. This shows the increase in the dominance of water soluble as the RH increases due to their hygroscopic growth.

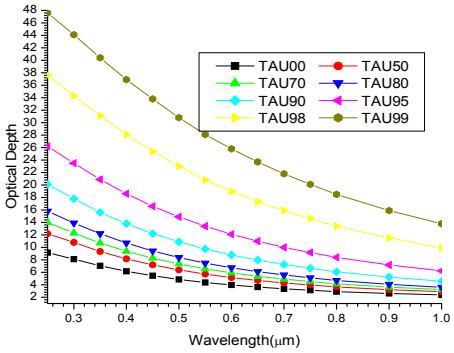

Figure 2b. A graph of optical depth against wavelength

Almost similar to that of figure 1b in relation to wavelength, but there is an increase in optical depths with respect to RHs..

LINEAR				QUADRATIC			
RH(%)	R^2	A	β	R^2	α_1	α_2	B
0	0.99726	1.01868	2.36092	0.99813	-1.12123	-0.07522	2.30869
50	0.99602	1.08026	2.93870	0.99891	-1.27885	-0.14568	2.81410
70	0.99486	1.09529	3.32283	0.99916	-1.34138	-0.18052	3.14914
80	0.99352	1.10162	3.75116	0.99935	-1.39000	-0.21154	3.52244
90	0.99043	1.09465	4.86592	0.99963	-1.45508	-0.26440	4.49797
95	0.98598	1.05941	6.76225	0.99983	-1.48834	-0.31466	6.15817
98	0.97864	0.97662	10.98435	0.99995	-1.46895	-0.36116	9.86572
99	0.97264	0.90531	15.42577	0.99998	-1.42381	-0.38035	13.77596

Table 3: The results of the Angstrom coefficients for Model2 using equations (4) and (5) at the respective relative humidities using regression analysis with SPSS16.0.

The change in α and α_2 is similar to table 2, but in this table there is a general increase in both the values with respect to all the RHs.

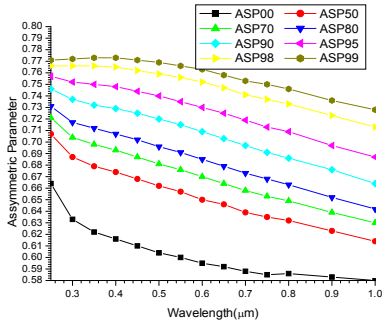

Figure 2c. A graph of asymmetric parameter against wavelength

Almost similar to that of figure 1c in relation to wavelength, but there is a slight increase with respect to RHs.

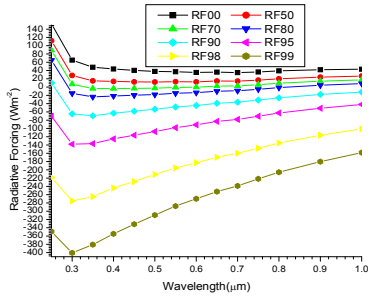

Figure 3a. A graph of radiative forcing against wavelength

It has similar behavior with that of 1a and 2a, but the main difference is that there is an increase in RF(warming) at 0 and 50% but at 70 no much change but as the RH increase we see that the forcing is decreasing as compared to figures 1a and 2a. This shows the increase in the dominance of water soluble as the RH increases. This shows that despite the fact that soot has higher particle density, but because is not water soluble so it is not affect by RH.

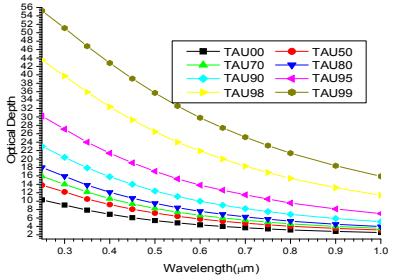

Figure 3b. A graph of optical depth against wavelength

Almost similar to that of figure 1b and 2b in relation to wavelength, but there is an increase in optical depths with respect to RHs.

Linear				Quadratic			
RH(%)	R^2	A	B	R^2	α_1	α_2	B
0	0.99693	1.05195	2.54593	0.99831	-1.18552	-0.09798	2.47281
50	0.99538	1.10884	3.22028	0.99903	-1.33826	-0.16830	3.06307
70	0.99413	1.12116	3.66811	0.99926	-1.39647	-0.20195	3.45429
80	0.99276	1.12457	4.16796	0.99945	-1.43995	-0.23135	3.89084
90	0.98955	1.11208	5.46798	0.99969	-1.49673	-0.28217	5.02786
95	0.98516	1.07151	7.67907	0.99985	-1.51862	-0.32799	6.96541
98	0.97801	0.98326	12.60398	0.99996	-1.48649	-0.36916	11.29351
99	0.97205	0.90971	17.78308	0.99999	-1.43659	-0.38650	15.85215

Table 4: The results of the Angstrom coefficients for Model3 using equations (4) and (5) at the respective relative humidities using regression analysis with SPSS16.0.

The changes in α and α_2 are similar to tables 2 and 3, but in this table there is a general increase in both the values with respect to all the RHs.

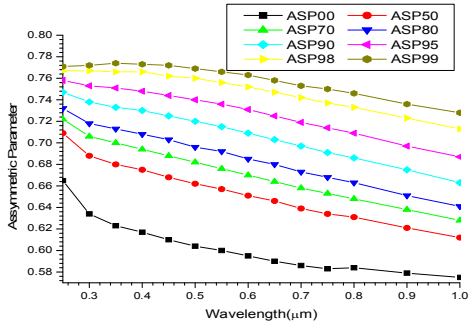

Figure 3c. a graph of asymmetric parameter against wavelength

Almost similar to that of figure 1c and 2c in relation to wavelength, but there is a slight increase in with respect to RHs.

		Model1		Model2		Model3	
RH(%)	Componennts	Volume Mix Ratio	Mass Mix Ratio	Volume Mix Ratio	Mass Mix Ratio	Volume Mix Ratio	Mass Mix Ratio
0	Inso	0.41380	0.47010	0.37600	0.42880	0.34450	0.39410
	Waso	0.43310	0.44290	0.47230	0.48470	0.50490	0.51980
	Soot	0.15310	0.08695	0.15170	0.08651	0.15060	0.08614
50	Inso	0.29890	0.38650	0.26500	0.34660	0.23790	0.31420
	Waso	0.59060	0.54210	0.62820	0.58350	0.65810	0.61710
	Soot	0.11050	0.07143	0.10690	0.06989	0.10390	0.06864
70	Inso	0.25560	0.34770	0.22450	0.30950	0.20010	0.27890
	Waso	0.64990	0.58800	0.68500	0.62810	0.71250	0.66020
	Soot	0.09447	0.06426	0.09051	0.06240	0.08742	0.06091
80	Inso	0.22140	0.31410	0.19300	0.27780	0.17110	0.24900
	Waso	0.69680	0.62780	0.72910	0.66620	0.75410	0.69670
	Soot	0.08182	0.05805	0.07783	0.05600	0.07475	0.05437
90	Inso	0.16670	0.25540	0.14370	0.22330	0.12630	0.19830
	Waso	0.77170	0.69750	0.79840	0.73170	0.81850	0.75840
	Soot	0.06160	0.04718	0.05794	0.04500	0.05516	0.04331
95	Inso	0.11980	0.19640	0.10230	0.16980	0.08924	0.14950
	Waso	0.83590	0.76730	0.85650	0.79600	0.87180	0.81780
	Soot	0.04427	0.03629	0.04124	0.03422	0.03898	0.03265
98	Inso	0.07567	0.13290	0.06402	0.11350	0.05549	0.09909
	Waso	0.89640	0.84250	0.91020	0.86360	0.92030	0.87930
	Soot	0.02796	0.02456	0.02581	0.02289	0.02424	0.02164
99	Inso	0.05526	0.10030	0.04657	0.08519	0.04024	0.07401
	Waso	0.92430	0.88110	0.93470	0.89760	0.94220	0.90980
	Soot	0.02042	0.01854	0.01878	0.01717	0.01757	0.01616

Table 5: Values of the Volume Mix Ratio and Mass Mix Ratio of aerosols compositions at the eight RHs.

From the table it can be observed that despite the fact that initially soot is 4 times more than the WS number concentration, it can be observed that the volume mix and mass mix ratios for WS are higher. It can also be observed that the difference in the volume mix and mass mix ratios is becoming higher with the increase in RHs.

CONCLUSIONS

So therefore we can say that the reason why the RF(warming) is increasing at 0 and 50 is because absorption by soot is dominant compared to scattering but by water soluble, but as the RH increases we noticed a decrease in warming. This is because as the RH increases since the soot particles are small and non hygroscopic, they therefore act as cloud condensation nuclei and so aid in the formation of clouds and therefore more scattering than absorption which now results in the cooling (Rosenfeld, 2006).

Additionally from table 5, it can be observed that as the RH increases the volume and mass mix ratios for water soluble are higher than that of soot and this difference is even more noticeable as the RH is increased because soots are non-hygroscopic and lighter than water soluble that are heavier and very hygroscopic.

This is also in line with what Haywood et. al., (1997) and Hansen et al., (1997) said, that a mixture of soot and WS depending on their compositions, can cause either cooling or warming of the atmosphere, thought we can add that depending also on RH.

REFERENCES

1. Alados-Arboledas, A., Alc´antara, A., Olmo, F. J., Mart´ınez-Lozano, J. A., Estell´es, V., Cachorro, V., Silva, A. M., Horvath, H., Gangl, A., D´ıaz, A., Pujadas, M., Lorente, J., Labajo, A., Sorribas, M., and Pavese, G.(2008): Aerosol columnar properties retrieved from Cimel radiometers during VELETA 2002, Atmos. Environ., 42, 2630–2642.
2. Alados-Arboledas, L., Lyamani, H., and Olmo, F. J.(2003): Aerosol size properties at Armilla, Granada (Spain), Q. J. Roy. Meteor. Soc., 129, 1395–1413.
3. Ångström, A.K. (1961). Techniques of Determining the Turbidity of the Atmosphere. Tellus XIII: 214.
4. Babu, S.S. and Moorthy, K.K. (2002). Aerosol Black Carbon over a Tropical Station in India. Geophys. Res. Lett. 29: L2098, doi: 10.1029/2002GL015662.
5. Bergin, M., Greenwald, R., Xu, J., Berta, Y. and Chemeides, W.L. (2001). Influence of Aerosol Dry Deposition on Photosynthetically Active Radiation Available to Plants: A Case Study in the Yangtze Delta Region of China. Geophys. Res. Lett. 28: 3605–3608.
6. Brown, L.M., Harrison, R. M., Maynard, A. D and Maynard, R. I (2003) Ultrafine particles in the atmosphere, London: Imperial College press.
7. Cao, J.J., Zhu, C.S., Chow, J.C., Watson, J.G., Han, Y.M., Wang, G.H., Shen, Z.X. and An, Z.S. (2009). Black Carbon Relationships with Emission and Meteorology in Xi'an, China. Atmos. Res. 94: 194–202.

8. Carrico, C.M., Rood, M.J., Ogren, J.A., (1998): Aerosol light scattering properties at Cape Grim, Tasmania, during the First Aerosol Characterization Experiment (ACE 1), J. Geophys. Res ., 103, 16565-16574.
9. Carrico, C.M., Rood, M.J., Ogren, J.A., (1998): Aerosol light scattering properties at Cape Grim, Tasmania, during the First Aerosol Characterization Experiment (ACE 1), J. Geophys. Res ., 103, 16565-16574.
10. Chameides, W.L., Yu, H., Liu, S.C., Bergin, M., Zhou, X., Mearns, L., Wang, G., Kiang, C.S., Saylor, R.D., Luo, C., Huang, Y., Steiner, A. and Giorgi, F. (1999). Case Study of the Effects of Atmospheric Aerosols and Regional Haze on Agriculture: An Opportunity to Enhance Crop Yields in China through Emission Controls? Proc. Nat. Acad. Sci. U.S.A. 96: 13626–13633.
11. Charlson, R.J., Schwartz, S.E., Hales, J. M., Cess, R. D., Coakley, J. A., Hansen, J. E and Hotmann, D. J (1992) Climate forcing by anthropogenic aerosols, Science 255, 423-430
12. Chylek, P., and J. Wong (1995), Effect of absorbing aerosols on global radiation bud get, Geophys . Res. Lett. , 22(8), 929 – 931, doi: 10.1 029/95GL00800.
13. Dockery, D. W. and Pope, C. A. (1996): Epidemiology of acute health effects: summary of time-series, in: Particles in our air: concen-tration and health effects, edited by: Wilson, R. and Spengler, J. D., Harvard University Press, Cambridge, MA, USA, 123–147.
14. Dubovik, O., Holben, B., Eck, T. F., Smirnov, A., Kaufman, Y. J., King, M. D., Tanr´e, D., and Slutsker, I. (2002):Variability of absorption and optical properties of key aerosol types observed in world-wide locations, J. Atmos. Sci., 59(3), 590–608.
15. Eck T. F., Holben B. N., Reid J. S., Dubovik O., Smirnovm A., O'Neill N. T., Slutsker I., and Kinne S.,(2000) "An observational approach for determining aerosol surface radiative forcing: results from the first field phase of INDOEX," J. Geophys. Res. 105, 15347–15360.
16. Eck, T. F., Holben, B. N., Dubovic, O., Smirnov, A., Goloub, P., Chen, H. B., Chatenet, B., Gomes, L., Zhang, X. Y., Tsay, S. C., Ji, Q., Giles, D., and Slutsker, I.(2005): Columnar aerosol optical properties at AERONET sites in central eastern Asia and aerosol transport to the tropical mid-Pacific, J. Geophys. Res., 110, D06202, doi:10.1029/2004JD005274,.
17. Eck, T. F., Holben, B. N., Dubovic, O., Smirnov, A., Slutsker, I., Lobert, J. M., and Ramanathan, V.(2001a): Column-integrated aerosol optical properties over the Maldives during the northeast mon-soon for 1998–2000, J. Geophys. Res., 106, 28 555–28 566.
18. Eck, T. F., Holben, B. N., Reid, J. S., Dubovic, O., Smirnov, A., O'Neil, N. T., Slutsker, I., and Kinne, S.(1999): Wavelength dependence of the optical depth of biomass burning, urban, and desert dust aerosols, J. Geophys. Res., 104(D24), 31 333–31 349.
19. Eck, T. F., Holben, B. N., Reid, J. S., Dubovic, O., Smirnov, A., O'Neil, N. T., Slutsker, I., and Kinne, S. (1999): Wavelength dependence of the optical depth of biomass burning, urban, and desert dust aerosols, J. Geophys. Res., 104(D24), 31 333–31 349,.
20. Eck, T. F., Holben, B. N., Ward, D. E., Dubovic, O., Reid, J. S., Smirnov, A., Mukelabai, M. M., Hsu, N. C., O' Neil, N. T., and Slutsker, I.(2001b): Characterization of the optical properties of biomass burning aerosols in Zambia during the 1997 ZIBBEE field campaign, J. Geophys. Res., 106(D4), 3425–3448.
21. Eck, T. F., Holben, B. N., Ward, D. E., et al.(2003): Variability of biomass burning aerosol optical characteristics in southern Africa during SAFARI 2000 dry season campaign and a compari-son of single scattering albedo estimates from radiometric measurements, J. Geophys. Res., 108(D13), 8477, doi:10.1029/2002JD002321.
22. Fitzgerald, J. W. (1975) Approximation formulas for the equilibrium size of an aerosol particle as a function of its dry size and composition and ambient relative humidity. J. Appl. Meteorol., 14, 1044 –1049

23. Foster, P., Ramaswamy, V., Artaxo, P., Berntsen, T., Betts, R., Fa-hey, D. W., Haywood, J., Lean, J., Lowe, D. C., Myhre, G., Nganga, J., Prinn, R., Raga, G., Schulz, M., and Van Dorland, R.(2007): Changes in Atmospheric Constituents and in Radiative Forcing, in: Climate Change 2007: The Physical Science Basis, Contribution of Working Group I to the Fourth Assessment Report of the Intergovernmental Panel on Climate Change, edited by: Solomon, S., Qin, D., Manning, M., Chen, Z., Marquis, M. , Averyt, K. B., Tignor, M., and Miller, H. L., Cambridge University Press, Cambridge, United Kingdom and New York, NY, USA.
24. Garland, R. M., Ravishankara, A. R., Lovejoy, E. R., Tolbert, M. A., and Baynard, T. (2007): Parameterization for the relative humidity dependence of light extinction: Organic-ammonium sulfate aerosol, J. Geophys. Res.-Atmos., 112, D19303, doi:10.1029/2006JD008179.
25. Gelencser, A (2005) Carbonaceous Aerosol. Dodrecht, the Netherland spinger.
26. Hanel, G. (1976). The Properties of Atmospheric Aerosol Particles as Functions of Relative Humidity at Thermodynamic Equilibrium with Surrounding Moist Air. In Advances in Geophysics, Vol. 19,H. E. Landsberg and J.Van Mieghem, eds., Academic Press, New York, pp. 73–188.
27. Hansen, J., Sato, M., and Ruedy, R.(1997): Radiative forcing and climate response, J. Geophys. Res., 102(D6), 6831–6864.
28. Hansen, J.E. and Sato, M. (2001). Trends of Measured Climate Forcing Agents. Proc. Nat. Acad. Sci. U.S.A. 98: 14778–14783.
29. Haywood, J. and Boucher, O. (2000): Estimates of the direct and indi-rect radiative forcing due to tropospheric aerosols: a review, Rev. Geophys., 38, 513-543.
30. Haywood, J. M., Roberts, D. L., Slingo, A., Edwards, J. M and Shine, K (1997): General circulation model calculations of the direct radiative forcing by Anthropogenic sulphate and fossil fuel soot aerosols. Journal of climate, 10 1562-1577Heintzenberg, J.: Size-segregated measurements of particulate elemental carbon and aerosol light absorption at remote artic locations, Atmos. Environ., 16, 2461–2469, 1982.
31. Hess M., Koepke P., and Schult I (May 1998), Optical Properties of Aerosols and Clouds: The Software Package OPAC, Bulletin of the A merican Met. Soc. **79**, 5, p831-844.
32. Horvath, H.(1995): Estimation of the average visibility in central Europe, Atmos. Environ., 29, 241-246.
33. Intergovernmental Panel on Climate Change (IPCC) (2007). Climate Change 2007: The Scientific Basis, In Contribution of Working Group I to the Fourth Assessment Report of the Intergovernmental Panel on Climate Change , Solomon, S. (Ed.), Cambridge Univ. Press, New York.
34. IPCC (2007), Climate Change 2007:Th e Physical Science Basis . Contribution of Working Group I to the Fourth Assessment Report of the Intergovernmental Panel on Climate Change, edited by S. Solomon et al., Cambridge Univ. Press, Cambridge, U. K.
35. Jacobson, M. Z.(2001): Strong radiative heating due to the mixing state of black carbon in atmospheric aerosols, Nature, 409, 695–697.
36. Kaskaoutis D. G., Kambezidis H. D., Hatzianastassiou N., Kosmopoulos P. G., and Badarinath K. V. S. (2007a) Aerosol climatology: dependence of the Angstrom exponent on wavelength over four AERONET sites, Atmos. Chem. Phys. Discuss., 7, 7347–7397.
37. Kaskaoutis, D. G., Kambezidis, H. D., Hatzianastassiou, N., Kosmopoulos, P. G., & Badarinath, K. V. S. (2007b). Aerosol climatology: On the discrimination of aerosol types over four AERONET sites. Atmospheric Chemistry and Physical Discussion, 7,6357–6411.
38. Kaufman, Y. J., (1993) Aerosol optical thickness and atmospheric path radiance, J. Geophys. Res., 98, 2677-2992.
39. Kaufman, Y. J., Koren, I., Remer, L. A., Rosenfeld, D., and Rudich, Y.(2005): The effect of smoke, dust, and pollution aerosol on shallow cloud development over the Atlantic Ocean, Proceedings of the National Academy of Sciences of the United States of America, 102(32), 11207–11212.
40. Kim, K.H., Sekiguchi, K., Kudo, S. and Sakamoto, K., (2011). Characterisitics of Atmospheric Elemental Carbon (Char and Soot) in Ultrafine and Fine Particles in a Roadside Environmental, Japan. Aerosol Air Qual. Res. 11: 1–12.

41. King, M. D. and Byrne, D. M.(1976): A method for inferring total ozone content from spectral variation of total optical depth obtained with a solar radiometer, J. Atmos. Sci., 33, 2242–2251.
42. Kumar B. S. K., K. R., Balakrishnaiah G., Gopal K. Rama, Reddy R.R., Reddy L.S.S., Ahammed Y. N, Narasimhulu K., Moorthy K. K., Babu S. S. (2012), Potential Source Regions Contributing to Seasonal Variations of Black Carbon Aerosols over Anantapur in Southeast India., Aerosol and Air Quality Research, 12: 344–358, ISSN: 1680-8584 print / 2071-1409 online doi: 10.4209/aaqr.2011.10.0159
43. Kuś mierczyk-Michulec, J. (2009). Ångström coefficient as an indicator of the atmospheric aerosol type for a well- mixed atmospheric boundary layer: Part 1: Model development. Oceanologia , Vol. 51, p. 5-39 .
44. Liou K. N.(2002) An Introduction to Atmospheric Radiation, 2nd ed. Academic, San Diego, Calif.,.
45. Menon, S., Hansen, J.E., Nazarenko, L. and Luo, Y. (2002). Climate Effects of Black Carbon Aerosols in China and India. Sciece 297: 2250–2253.
46. Mikhailov, E. F., Vlasenko, S. S., Podgorny, I. A., Ramanathan, V., and Corrigan, C. E. (2006): Optical properties of soot-water drop agglomerates: An experimental study, J. Geophys. Res.-Atmos., 111, D07209, doi:10.1029/2005Jd006389.
47. Moorthy, K.K. and Babu, S.S. (2006). Aerosol Black Carbon over Bay of Bengal Observed from an Island Location, Port Blair: Temporal Features and Long Range Transport. J. Geophys. Res. 111: D17205. doi: 10.1029/2005JD006855.
48. Myhre, G., Stordal, F., Restad, K. and Isaksen, I.S.A. (1998). Estimation of the Direct Radiative Forcing Due to Sulfate and Soot Aerosols. Tellus Ser. B 50: 463–477.
49. O'Neill, N. and Royer, A.(1993): Extraction of bimodal aerosol size distribution radii from spectral and angular slope Angstrom coefficients, Appl. Opt., 32, 1642–1645.
50. O'Neill, N. T., Dubovic, O., and Eck, T. F.(2001a): Modified˚ Angstrom exponent for the characterization of submicrometer aerosols, Appl. Opt., 40(15), 2368–2375.
51. O'Neill, N. T., Eck, T. F., Holben, B. N., Smirnov, A., and Dubovic, O. (2001b): Bimodal size distribution influences on the variation of ˚ Angstr¨ om derivates in spectral and optical depth space, J. Geophys. Res., 106(D9), 9787–9806.
52. O'Neill, N. T., Eck, T. F., Smirnov, A., Holben, B. N., and Thulasiraman, S. (2003): Spectral dis-crimination of coarse and fine mode optical depth, J. Geophys. Res., 198(D17), 4559, doi:101029/2002JD002975.
53. Park, S.S., Kim, Y.J. and Fung, K. (2002). PM2.5 Carbon Measurements in Two Urban Areas: Seoul and Kwanglu, Korea. Atmos. Environ. 36: 1287–1297.
54. Penner, J. E., Dickinson, R. E. and O'Neil, C. A. (1992). Effects of aerosol from biomass burning on the global radiation budget. Science, 256, 1432-1434.
55. Ramanathan, V., Crutzen, P.J., Kiehl, J.T. and Rosenfield, D. (2001). Atmosphere: Aerosols, Climate, and the Hydrogical Cycle. Science 294: 2119–2124.
56. Rana S., Kant Y., Dadhwal V. K. (2009), Diurnal and Seasonal Variation of Spectral Properties of Aerosols over Dehradun, India Aerosol and Air Quality Research, Vol. 9, No. 1, pp. 32-49, 2009
57. Ranjan, R.R., Joshi, H.P. and Iyer, K.N. (2007). Spectral variation of total column aerosol optical depth over Rajkot: A tropical semi-arid Indian station. Aerosol Air Qual. Res. 7: 33-45.

58. Reddy, M.S. and Venkataraman, C. (1999). Direct Radiative Forcing from Anthropogenic Carbonaceous Aerosols over India. Curr. Sci. 76: 1005–1011.
59. Reid, S. J., Eck T. F., Christopher S. A., Hobbs P. V. and Holben B.,(1999) Use of Angtrom exponent to estimate the variability of optical and physical properties of aging smoke particles in Brazil, J. Geophys. Res. 104(D22), 27, 473—27, 489.
60. Rosenfeld, D. (2006). Aerosols, Clouds and Climate. Science 312: 1323-1324.
61. Salako, G.O., Hopke, P.K., Cohen, D.D., Begum, B.A., Biswas, S.K., Pandit, G.G., Chung, Y.S., Rahman, S.A., Hamzah, M.S., Davy, P., Markwitz, A., Shagjjamba, D., Lodoysamba, S., Wimolwattanapun, W. and Bunprapob, S. (2012). Exploring the Variation between EC and BC in a Variety of Locations. Aerosol Air Qual. Res. 12: 1–7.
62. Schuster, G. L., Dubovik, O., and Holben, B. N. (2006): Angstrom exponent and bimodal aerosol size distributions, J. Geophys. Res., 111, D07207, doi:101029/2005JD006328.
63. Schwartz, S. E., Arnold, F., Blanchet, J. P., Durke, P. A., Hofmann, D. J., Hoppel, W. A., King, M. D., Lacis, A. A., Nakajima, T., Ogren, J. A., Toon, O. B., and Wendisch, M. (1995): Group report: con-nections between aerosol properties and forcing of climate, in: Aerosol of Climate, edited by: Heintzenberg, J. and Charlson, R. J., Wiley, New York, 251–280.
64. Segan, C. and Pollack, J. (1967). Anisotropic nonconservative scattering and the clouds of Venus. J. Geophys. Res. 72, 469-477.
65. Seinfeld, J.H and Pandis, S.N (1998), Atmospheric Chemistry and Physics from air pollution to climate change, John Wiley, Hoboken, N.J
66. Tang, I. N. (1996). Chemical and size effects of hygroscopic aerosols on light scattering coefficients. Journal of Geophysical Research, 101, 19245–19250.
67. Viidanoja, J., Sillanpa, M., Laakia, J., Kerminen, V.M., Hillamo, R., Aarnio, P. and Koskentalo, T. (2002). Organic and Black Carbon in PM2.5 and PM10: 1 Year Data from an Urban Site in Helsinki, Finland. Atmos. Environ. 36: 3183–3193.
68. Waggoner, A. P., Weiss, R. E., Ahlquist, N. C., Covert, D. S., Will, S., and Charlson, R. J. (1981): Optical characteristics of atmospheric aerosols, Atmos. Environ., 15, 1891–1909.